

Unsteady Wave Drag on a Disturbance Moving Along an Arbitrary Trajectory

Lucas Gierczak-Galle,^{1,2} Assil Fadle,^{1,3} Maxence Arutkin,² Elie Raphaël,² and Michael Benzaquen³

¹*Ecole Normale Supérieure, 45 rue d'Ulm, 75005 Paris, France*

²*UMR CNRS 7083 Gulliver, ESPCI Paris, PSL Research University, 75005 Paris, France*

³*UMR CNRS 7646 LadHyX, Ecole polytechnique, 91128 Palaiseau Cedex, France*

(Dated: March 2, 2022)

We derive analytical formulas for the wake and wave drag of a disturbance moving arbitrarily at the air-water interface. We show that, provided a constant velocity is reached in finite time, the unsteady surface displacement converges to its well-known steady counterpart as given by Havelock's famous formula. Finally we assess, in a specific situation, to which extent one can rightfully use Havelock's steady wave drag formula for non-uniform motion (quasi-static). Such an approach can be used to legitimize or discredit a number of studies which used steady wave drag formulas in unsteady situations.

I. INTRODUCTION

Water waves have fascinated physicists and mathematicians for centuries. Among them, Lagrange was the first to derive the governing equations [1, 2] and Kelvin to account successfully for the famous V-shape pattern of the wake behind a ship using stationary phase arguments [3]. Kelvin's theory was recently brought up to date thanks to airborne observations of ship wakes [4, 5], revealing more intricate phenomena which would not have been observable back in the day.

The wake of a moving disturbance, say, a ship, naturally carries energy radiated by the source. Such energy loss translates into a drag force exerted on the disturbance and opposing its motion, commonly called *wave drag* or *wave resistance* [6]. Both Havelock [7] and Michell [8] proposed methods to compute the wave drag of a body moving steadily at the air-water interface, which have been extensively used by both physicists and naval engineers in the shipbuilding industry [2, 9] throughout the past century. Numerous experimental and theoretical studies have focused on the extension of their results to account for the aspect ratio of the body [10, 11], its front-back asymmetry [12], or varying depth [13] with applications for hull design and rowing sports to name a few. At smaller scales, where capillarity is no longer negligible, the analysis of the wave drag is also relevant [14], notably to understand the biolocomotion of certain insects and beetles [15–17]. The highly unsteady nature of the propulsion mechanisms of such insects revealed the importance of being able to properly account for unsteady effects in the wave drag [18].

Lacking a general formula to compute the wave drag for unsteady motion, a number of studies have used the steady Havelock formula as if it were applicable, see e.g. [13, 19]. While in some cases (likely quasi-static) this might be justified, one may rightfully argue that it will lead to inaccurate conclusions in others.

In the present paper, we extend Havelock's theory to compute the unsteady wake and wave drag of disturbance with given trajectory $\mathbf{r}_0(t) = (x_0(t), y_0(t))$, which has no other constraints than being smooth enough, typically \mathcal{C}^1 , see below. We obtain a general formula for both pure gravity, and capillary-gravity waves allowing to compute the wake and wave drag for any $\mathbf{r}_0(t)$. We illustrate our results for uniformly accelerated motion, which allows to determine an acceleration threshold below which Havelock's steady wave drag formula can be considered accurate to some extent. See also the interesting study by Dutykh & Dias [20] for an analysis of the unsteady waves generated by a moving bottom.

II. UNSTEADY WAKES

In this section we derive the surface elevation caused by a moving disturbance at the air-water interface. We assume irrotational flow of an inviscid and infinitely deep fluid of constant and uniform density ρ , extending infinitely in the (x, y) plane. The surface elevation of the fluid is denoted $\zeta(\mathbf{r}, t)$ with $\mathbf{r} = (x, y)$. Following

Havelock's method, the moving disturbance is modeled by an external pressure field $P_{\text{ext}}(\mathbf{r}, t)$ applied to the fluid surface, on top of the atmospheric pressure P_{atm} .

Hereafter we shall restrict to a linearized setting in which the waves amplitude always remain small compared to the wavelength, allowing to neglect second-order terms and make extensive use of Fourier transform. The disturbance trajectory is given by $\mathbf{r}_0(t)$, assumed to be smooth enough (typically \mathcal{C}^1), such that:

$$P_{\text{ext}}(\mathbf{r}, t) = P_e(\mathbf{r} - \mathbf{r}_0(t)), \quad (1)$$

with $P_e(\mathbf{r})$ the pressure field at $t = 0$ at position \mathbf{r} . Denoting by $\hat{\cdot}$ the two-dimensional Fourier Transform with respect to \mathbf{r} , it follows that:

$$\hat{P}_{\text{ext}}(\mathbf{k}, t) = \hat{P}_e(\mathbf{k})e^{-i\mathbf{k} \cdot \mathbf{r}_0(t)}. \quad (2)$$

Denoting \mathbf{u} the velocity field in the fluid, the linearized Euler equations read:

$$\partial_t \mathbf{u} = -\nabla P / \rho + \mathbf{g}, \quad (3a)$$

$$\nabla \cdot \mathbf{u} = 0, \quad (3b)$$

where \mathbf{g} denotes the acceleration of gravity. Combining $\nabla \times \mathbf{u} = \mathbf{0}$ with Eq. (3b) yields that the scalar velocity potential ϕ , defined as $\mathbf{u} = \nabla \phi$ satisfies the Laplace equation:

$$\Delta \phi = 0. \quad (4)$$

Equations (3) and (4) need to be complemented by the linearized boundary conditions at $z = \zeta$:

$$\partial_t \zeta = \partial_z \phi|_{z=\zeta}, \quad (5a)$$

$$P|_{z=\zeta} = P_{\text{atm}} + P_{\text{ext}} - \gamma \Delta_{x,y} \zeta, \quad (5b)$$

respectively called kinematic and dynamical boundary conditions, and where γ is the surface tension. Combining Eqs (2) to (5) with some Fourier analysis yields a second-order ordinary linear differential equation in time for the Fourier Transform of the surface elevation $\hat{\zeta}(\mathbf{k}, t)$ (see e.g. [14, 21]):

$$\partial_t^2 \hat{\zeta}(\mathbf{k}, t) + \omega(k)^2 \hat{\zeta}(\mathbf{k}, t) = -\frac{1}{\rho} k \hat{P}_e(\mathbf{k}) e^{-i\mathbf{k} \cdot \mathbf{r}_0(t)}, \quad (6)$$

with $\omega(k)^2 = gk + \gamma k^3 / \rho$. Choosing as initial condition that the disturbance is turned on at $t = 0$ (which implies that $\zeta = 0$ beforehand):

$$\hat{\zeta}(\mathbf{k}, t = 0) = 0, \quad (7a)$$

$$\partial_t \hat{\zeta}(\mathbf{k}, t = 0) = 0, \quad (7b)$$

one obtains a general solution of Eq. (6) which holds for all trajectories $\mathbf{r}_0(t)$ (see Appendix A for the details):

$$\hat{\zeta}(\mathbf{k}, t) = - \int_0^t \sin(\omega(k)(t - \tau)) \frac{k \hat{P}_e(\mathbf{k}) e^{-i\mathbf{k} \cdot \mathbf{r}_0(\tau)}}{\rho \omega(k)} d\tau. \quad (8)$$

In the case of linear motion considered in Closa *et al.* [21] in which the disturbance undergoes uniform linear straight motion $\mathbf{r}_0(t) = r_0(t) \mathbf{u}_x$ with $r_0(t) = vt$ starting at $t = 0$, one can show that the wake converges to the well-known Havelock steady wave pattern. Using Eq. (8) one obtains the surface elevation $\hat{\zeta}_d(\mathbf{k}, t)$ in the frame of reference attached to the moving disturbance (see Appendix B for the details):

$$\hat{\zeta}_d(\mathbf{k}, t) = -\frac{k \hat{P}_e(\mathbf{k})}{\rho \omega(k)} \frac{1}{\omega(k)^2 - (vk_x)^2} \left[\omega(k) - e^{ivk_x t} \cos(\omega(k)t) \omega(k) + i e^{ivk_x t} \sin(\omega(k)t) vk_x \right]. \quad (9)$$

Breaking up the cosine and sine functions into terms of the form $e^{\pm i\omega t}$, one can write $\hat{\zeta}_d(\mathbf{k}, t)$ as the sum of five terms $\hat{\zeta}_{d,j}(\mathbf{k}, t)$ for $j \in [1, 5]$, the first one ($j = 1$) being the constant one while the four others are oscillating

functions of time. Noticing incidentally that $\hat{\zeta}_{d,1}(\mathbf{k}, t) = \hat{\zeta}_{st}(\mathbf{k})$, the well-known steady wave pattern, see e.g. [14, 21]:

$$\hat{\zeta}_{st}(\mathbf{k}) = -\frac{1}{\rho} \frac{k \hat{p}_e(\mathbf{k})}{\omega(k)^2 - (vk_x)^2}. \quad (10)$$

To prove that the unsteady wake converges to its steady counterpart, one then needs to prove that the four other contributions vanish as $t \rightarrow +\infty$. In Appendix C, we show that for all $j \geq 2$, $\zeta_{d,j}(\mathbf{r}, t) \rightarrow 0$, and as a result $\zeta_d(\mathbf{r}, t) \rightarrow \zeta_{st}(\mathbf{r})$.

Such results extend to any linear motion for which a constant final velocity is reached in finite time, see Appendix C. A more realistic trajectory would indeed consist of an acceleration phase during which the velocity smoothly increases until it reaches a cruising plateau.

III. UNSTEADY WAVE DRAG

As mentioned above, the energy transferred to the waves translates into a drag force exerted on the disturbance and opposing its motion. In the case of steady motion and according to Havelock's reasoning in [7], the wave drag \mathbf{R}_w is given by the total resolved pressure in the direction of the motion $P_e d\mathbf{S} \cdot \mathbf{m}$ where \mathbf{m} is the unit vector collinear to the velocity, and $d\mathbf{S}$ the surface element vector orthogonal to the air-water interface. Using that $d\mathbf{S} \cdot \mathbf{m} = (\mathbf{m} \cdot \nabla) \zeta dS$, one obtains Havelock's formula:

$$\mathbf{R}_w = - \iint P_e (\mathbf{m} \cdot \nabla) \zeta dS. \quad (11)$$

Such a result can also be obtained from a simple energy balance. The power transferred to the waves by the moving disturbance writes [6]:

$$\mathcal{P} = \iint P_e \nabla_n \phi dS, \quad (12)$$

with ∇_n denoting the derivative along the vector normal to the surface. Noting that $\nabla_n \phi = \mathbf{v} \cdot \nabla \zeta$ where $\mathbf{v} = \partial_t \mathbf{r}_0$, and matching \mathcal{P} to the power of a force acting against the motion, $\mathcal{P} = -\mathbf{R}_w \cdot \mathbf{v}$, yields Eq. (11).

Extending such reasoning to the unsteady setting in which the surface elevation is time-dependent yields a nonzero vertical component. Using Havelock's approach, the horizontal component is given as before by:

$$\mathcal{P}_w(t) = - \iint P_e (\mathbf{v} \cdot \nabla) \zeta dS. \quad (13)$$

The power of the vertical component can, on the other hand, be computed by noting that the infinitesimal vertical work of the pressure field on the surface between t and $t + dt$ is given by $\delta W_v = -P_e dz$ with $dz = \partial_t \zeta(x, y, t) dt$ the infinitesimal vertical displacement of the surface. The vertical power thus reads:

$$\mathcal{P}_v(t) = - \iint P_e \partial_t \zeta dS. \quad (14)$$

This term naturally vanishes in the steady case ($\partial_t \zeta = 0$). Multiplying the kinematic boundary condition in the frame of reference of the moving disturbance $\partial_t \zeta + (\mathbf{v} \cdot \nabla) \zeta = \partial_z \phi$ by P_e and integrating over the surface, one sees that the overall power transferred to the waves matches the power of the vertical and horizontal forces acting on the moving disturbance: $\mathcal{P} = -(\mathcal{P}_w + \mathcal{P}_v)$, with $\mathcal{P}(t)$ given by Eq. (12).

In summary, for an arbitrarily moving disturbance the power transferred to the waves translates into a force with a vertical and a horizontal components. The horizontal one is what we call wave drag (at standstill, the

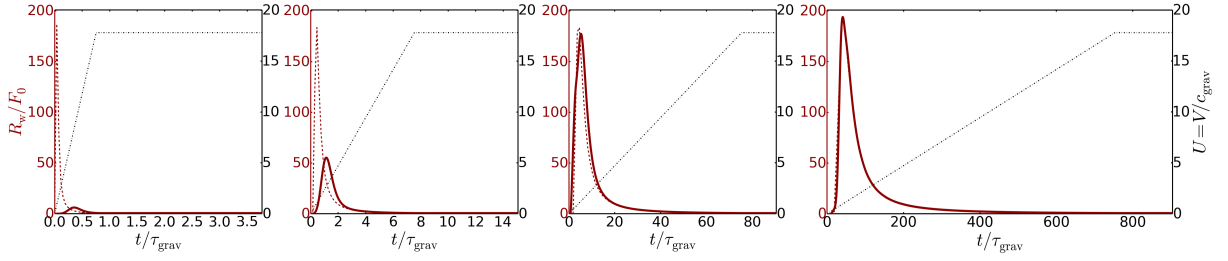


FIG. 1. Pure gravity instantaneous wave drag (dark red curves and left vertical axis) experienced by a moving disturbance for four different values of the acceleration – from left to right: $a \approx 230, 23, 2.3$ and $0.23 \text{ m}\cdot\text{s}^{-2}$ – as function of time rescaled by $\tau_{\text{grav}} = \sqrt{b/g}$. The dashed dark red line shows the wave drag computed from Havelock’s steady wave drag formula. The dash-dotted black line signifies the velocity profile rescaled by $c_{\text{grav}} = \sqrt{g b}$ (right vertical axis).

moving disturbance does not experience any drag, only vertical oscillations [21]). Combining Eq. (11) with Eq. (8) yields:

$$\mathbf{R}_w = \frac{\mathbf{m}}{4\pi^2} \iint d^2\mathbf{k} \frac{ik|\hat{P}_e(\mathbf{k})|^2(\mathbf{k}\cdot\mathbf{m})}{\rho\omega(k)} \int_0^t d\tau \sin(\omega(k)(t-\tau)) e^{ik(\mathbf{r}_0(t)-\mathbf{r}_0(\tau))}, \quad (15)$$

where we recall that \mathbf{m} is the unit vector collinear to the velocity. Eq. (15) is the central result of this paper. It gives the instantaneous wave drag for any trajectory $\mathbf{r}_0(t)$ with nonzero velocity. In the particular case of linear motion, and axis-symmetric pressure disturbance, $\hat{P}_e(\mathbf{k}) = \hat{P}_e(k)$, Eq. (15) simplifies to:

$$\mathbf{R}_w = -\frac{\mathbf{m}}{2\pi} \int_0^\infty dk \frac{k^3|\hat{P}_e(k)|^2}{\rho\omega(k)} \int_0^t d\tau \sin(\omega(k)(t-\tau)) J_1(k(r_0(t)-r_0(\tau))), \quad (16)$$

where J_1 denotes the Bessel function of the first kind and of order 1. Note that in the case of a linear sudden object motion described above one recovers the results of Closa *et al.* [21]. Also note that in the more general case of linear motion with constant final velocity reached in finite time, having shown that the wake pattern in the disturbance’s frame of reference converges to a constant, the same is true concerning wave drag.

IV. HOW SLOW IS SLOW ENOUGH?

In this section we raise the question of the accuracy of using Havelock’s steady formula to compute the wave drag in an unsteady situation. In other words, how small does the acceleration need to be for the evolution to be reasonably considered as quasi-static wave drag-wise. To answer this question in a stylized setting, we compute $R_w(t)$ for various different velocity profiles. More precisely we choose a ramp velocity profile with constant acceleration of the form $\mathbf{r}_0(t) = \frac{1}{2}at^2\mathbf{u}_x$.

Figure 1 shows the result in the pure gravity limit, $\omega(k)^2 = gk$, for four values of the acceleration a , computed with a Lorentzian pressure field of the form $\hat{P}_e(k) = F_0 e^{-b|k|}$, where b is the typical size of the disturbance. One can see that, as expected, the quasi-steady limit is achieved for $a \ll g$.

Figure 2 shows the results for capillary-gravity waves for three values of the final velocity v_∞ and four values of the velocity ramp’s duration t_{ramp} . We choose $b = \kappa^{-1}/10$, with $\kappa^{-1} = \sqrt{\gamma/(\rho g)}$ the capillary length, to ensure that capillary effects are non-negligible [22]. While we consistently find again that the instantaneous wave drag coincides better and better with its steady counterpart as the acceleration is decreased, significant oscillations remain, at odds with the pure gravity case. The three rows describe three physically different regimes of final velocities, see [21]. For $v_\infty < c_{\text{min}}$, the final wave drag is zero, whereas it is non-zero whenever $v_\infty \geq c_{\text{min}}$. Further, while for $v_\infty < c_{\text{crit}} \approx 0.77c_{\text{min}}$ the oscillations decay exponentially, for $v_\infty > c_{\text{crit}}$ they decay as $1/t$.

Also note that even for the weakest acceleration (bottom right panel in Fig. 2), the discontinuity of wave drag in the capillary-gravity case expected to occur at $U/c_{\text{min}} = 0.23$, as computed by Raphaël & de Gennes [14], is

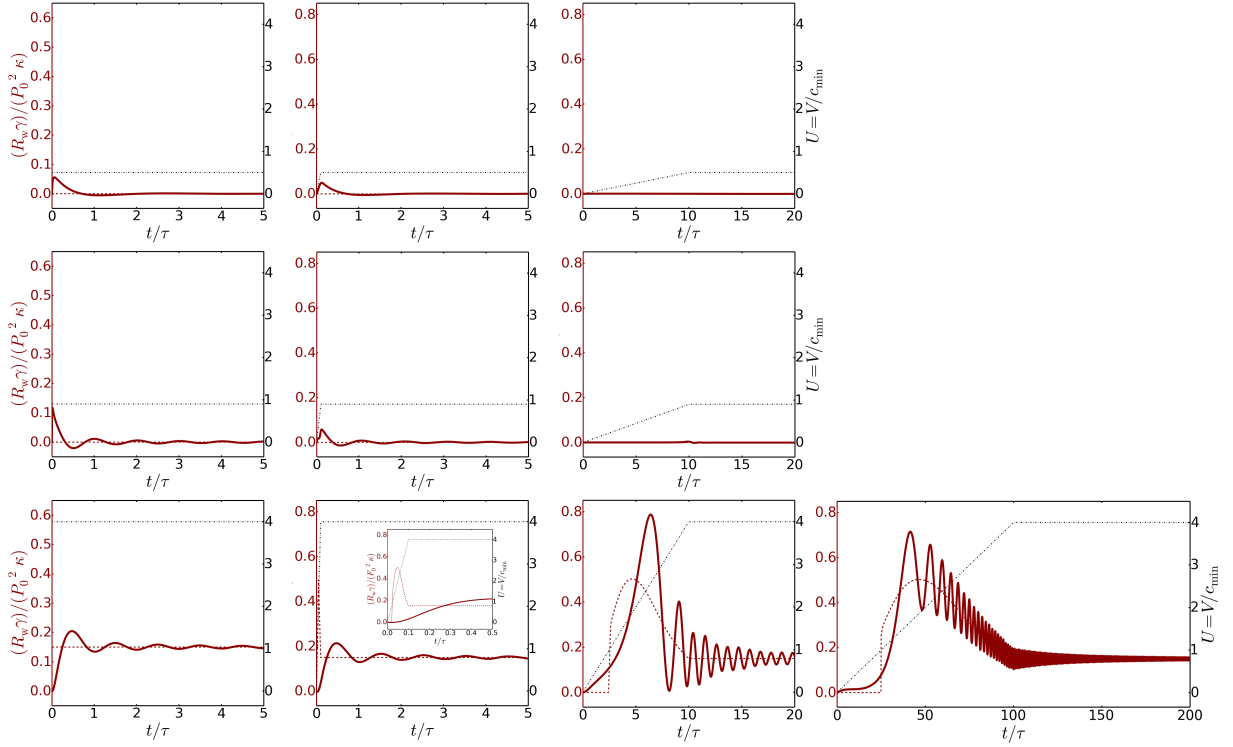


FIG. 2. Capillary-gravity instantaneous wave drag (dark red curves and left vertical axis) experienced by a moving disturbance for three values of the final velocity – from top to bottom: $v_\infty/c_{\min} = 0.5, 0.9$ and 4 where $c_{\min} = (4g\rho/\gamma)^{1/4} \approx 0.23 \text{ m}\cdot\text{s}^{-1}$ – and four different durations of the velocity ramp. – from left to right: $t_{\text{ramp}} = 0$ (constant velocity), $\tau/10$, 10τ and 100τ where τ is the pseudo-period of oscillations. The corresponding accelerations are, from left to right: for $v_\infty/c_{\min} = 0.5$, $a \approx \infty, 13$ and $0.13 \text{ m}\cdot\text{s}^{-2}$; for $v_\infty/c_{\min} = 0.9$, $a \approx \infty, 2.5$ and $0.025 \text{ m}\cdot\text{s}^{-2}$; for $v_\infty/c_{\min} = 4$, $a \approx \infty, 2300, 23$ and $2.3 \text{ m}\cdot\text{s}^{-2}$. The dashed dark red line shows the wave drag computed from Havelock’s steady wave drag formula. The dash-dotted black line signifies the velocity profile rescaled c_{\min} (right vertical axis). The two seemingly missing panels have been left out as they require unnecessary computing power, in addition to being almost perfectly flat lines at $R_w = 0$.

phased out in the unsteady case. This could be a solution to the apparent contradiction with the experimental results of Burghlea & Steinberg [23, 24], who claimed that such discontinuity did not exist. See also [25] and [22] for alternative explanations.

V. CONCLUSION

In this paper we have derived a general formula to compute the instantaneous wave drag exerted on an arbitrarily moving disturbance. In particular, we have assessed in a specific situation to which extent one can rightfully use Havelock’s steady wave drag formula. Such an approach can be used to legitimize or discredit a number of studies which used steady wave drag formulas in unsteady situations, see e.g. [13, 19].

Of particular interest is the experimental analysis of Le Merrer *et al.* [19] in which the capillary-gravity wave drag was inferred from the free deceleration of a liquid nitrogen droplet launched over the water surface [19]. The discrepancies observed by the authors between the experiments and the theoretical steady wave drag could perhaps be attributed to the fact that their experiments did not fall in the quasi-static regime in which steady Havelock is accurate. To solve this free deceleration problem one needs to compute jointly the wave drag (Eq. (16)) and the resulting dynamics of the moving disturbance (the nitrogen droplet) from Newton’s law: $m\ddot{r}_0 = -\beta\dot{r}_0 - R_w(\{r_0(t)\})$, with m the mass of the liquid nitrogen droplet and β a friction coefficient. Further, computing the average wave drag for an oscillating velocity profile of the form $v(t) = v_0(1 + \varepsilon \sin \Omega t)$

would be highly relevant to address optimal strategies in rowing sports, see [26, 27]. Such studies are left for future work.

We thank C. Clanet, A. Darmon, U. Mizrahi and F. Vandenbrouck for fruitful discussions. We also thank Z. Zeravcic for her help with the numerical computations, and R. Carmigniani for his thorough proofreading.

-
- [1] Olivier Darrigol, *Worlds of flow: A history of hydrodynamics from the Bernoullis to Prandtl* (Oxford University Press, 2005).
 - [2] J Lighthill, *Waves in Fluids* (1978) p. 120.
 - [3] Lord Kelvin, “On ship waves,” *Proc. Inst. Mech. Eng* **3**, 409–434 (1887).
 - [4] Marc Rabaud and Frédéric Moisy, “Ship wakes: Kelvin or Mach angle?” *Physical Review Letters* **110**, 214503 (2013).
 - [5] Alexandre Darmon, Michael Benzaquen, and Élie Raphaël, “Kelvin wake pattern at large Froude numbers,” *Journal of Fluid Mechanics* **738** (2014).
 - [6] John V Wehausen and Edmund V Laitone, “Surface waves,” in *Fluid Dynamics/Strömungsmechanik* (Springer, 1960) pp. 446–778.
 - [7] TH Havelock, “The theory of wave resistance,” *Proceedings of the Royal Society of London. Series A, Containing Papers of a Mathematical and Physical Character* **138**, 339–348 (1932).
 - [8] John Henry Michell, “Xi. the wave-resistance of a ship,” *The London, Edinburgh, and Dublin Philosophical Magazine and Journal of Science* **45**, 106–123 (1898).
 - [9] Kevin E Parnell and Henrik Kofoed-Hansen, “Wakes from large high-speed ferries in confined coastal waters: Management approaches with examples from New Zealand and Denmark,” *Coastal Management* **29**, 217–237 (2001).
 - [10] Michael Benzaquen, Alexandre Darmon, and Élie Raphaël, “Wake pattern and wave resistance for anisotropic moving disturbances,” *Physics of Fluids* **26**, 092106 (2014).
 - [11] Jean-Philippe Boucher, Romain Labbé, Christophe Clanet, and Michael Benzaquen, “Thin or bulky: Optimal aspect ratios for ship hulls,” *Physical Review Fluids* **3**, 074802 (2018).
 - [12] GP Benham, Jean-Philippe Boucher, Romain Labbé, Michael Benzaquen, and Christophe Clanet, “Wave drag on asymmetric bodies,” *Journal of Fluid Mechanics* **878**, 147–168 (2019).
 - [13] GP Benham, R Bendimerad, M Benzaquen, and C Clanet, “Hysteretic wave drag in shallow water,” *arXiv preprint arXiv:2003.00502* (2020).
 - [14] E. Raphaël and P-G. De Gennes, “Capillary gravity waves caused by a moving disturbance: wave resistance,” *Physical Review E* **53**, 3448 (1996).
 - [15] Jonathan Voise and Jérôme Casas, “The management of fluid and wave resistances by whirligig beetles,” *Journal of The Royal Society Interface* **7**, 343–352 (2010).
 - [16] David L Hu, Brian Chan, and John WM Bush, “The hydrodynamics of water strider locomotion,” *Nature* **424**, 663–666 (2003).
 - [17] Oliver Bühler, “Impulsive fluid forcing and water strider locomotion,” *Journal of Fluid Mechanics* **573**, 211–236 (2007).
 - [18] Thomas Steinmann, Maxence Arutkin, Précillia Cochard, Élie Raphaël, Jérôme Casas, and Michael Benzaquen, “Unsteady wave pattern generation by water striders,” *Journal of Fluid Mechanics* **848**, 370–387 (2018).
 - [19] Marie Le Merrer, Christophe Clanet, David Quéré, Élie Raphaël, and Frédéric Chevy, “Wave drag on floating bodies,” *Proceedings of the National Academy of Sciences* **108**, 15064–15068 (2011).
 - [20] Denys Dutykh and Frédéric Dias, “Water waves generated by a moving bottom,” in *Tsunami and Nonlinear waves* (Springer, 2007) pp. 65–95.
 - [21] Fabien Closa, AD Chepelienskii, and Élie Raphaël, “Capillary-gravity waves generated by a sudden object motion,” *Physics of Fluids* **22**, 052107 (2010).
 - [22] Michael Benzaquen, Frédéric Chevy, and Élie Raphaël, “Wave resistance for capillary gravity waves: Finite-size effects,” *EPL (Europhysics Letters)* **96**, 34003 (2011).
 - [23] Teodor Burghilea and Victor Steinberg, “Wave drag due to generation of capillary-gravity surface waves,” *Physical Review E* **66**, 051204 (2002).
 - [24] Teodor Burghilea and Victor Steinberg, “Onset of wave drag due to generation of capillary-gravity waves by a moving object as a critical phenomenon,” *Physical review letters* **86**, 2557 (2001).
 - [25] Denis Richard and Elie Raphael, “Capillary-gravity waves: The effect of viscosity on the wave resistance,” *EPL (Europhysics Letters)* **48**, 49 (1999).
 - [26] Jean-Philippe Boucher, Romain Labbé, and Christophe Clanet, “Row bots,” *Physics Today* **70**, 82 (2017).
 - [27] Romain Labbé, Jean-Philippe Boucher, Christophe Clanet, and Michael Benzaquen, “Physics of rowing oars,” *New Journal of Physics* **21**, 093050 (2019).

Appendix A: Unsteady wake solution

Our aim here is to solve Eq. (6): $\rho(\partial_t^2 \hat{\zeta}(\mathbf{k}, t) + \omega(k)^2 \hat{\zeta}(\mathbf{k}, t)) = -k \hat{P}_e(\mathbf{k}) e^{-i\mathbf{k} \cdot \mathbf{r}_0(t)}$, with the initial conditions (7a) and (7b). One readily notices that we have an explicit basis of the solution space at our disposal: $y_1(t) = e^{i\omega(k)t}$ and $y_2(t) = e^{-i\omega(k)t}$. One can therefore look for solutions of the form:

$$\hat{\zeta}(\mathbf{k}, t) = \lambda(t)y_1(t) + \mu(t)y_2(t), \quad (\text{A1})$$

λ and μ being two smooth functions of class \mathcal{C}^1 which depend on \mathbf{k} implicitly. One can find the exact solution under the prescribed initial conditions by solving the system:

$$\begin{pmatrix} y_1 & y_2 \\ y_1' & y_2' \end{pmatrix} \begin{pmatrix} \lambda' \\ \mu' \end{pmatrix} = \begin{pmatrix} 0 \\ -\frac{k \hat{P}_{\text{ext}}(\mathbf{k}) e^{-i\mathbf{k} \cdot \mathbf{r}_0(t)}}{\rho} \end{pmatrix}, \quad (\text{A2})$$

Upon identification and integration, one is left with:

$$\hat{\zeta}(\mathbf{k}, t) = \left(c(\mathbf{k}) - \frac{k}{2i\omega(k)\rho} \int_0^t e^{-i\omega(k)\tau} \hat{P}_e(\mathbf{k}, \tau) d\tau \right) e^{i\omega(k)t} + \left(d(\mathbf{k}) + \frac{k}{2i\omega(k)\rho} \int_0^t e^{i\omega(k)\tau} \hat{P}_e(\mathbf{k}, \tau) d\tau \right) e^{-i\omega(k)t}. \quad (\text{A3})$$

The initial conditions (7a) and (7b) yield that $c(\mathbf{k}) = d(\mathbf{k}) = 0$, and consequently Eq. (8).

Appendix B: The case of sudden uniform linear motion

In the case of a sudden uniform linear motion, the expression of $\hat{\zeta}$ reduces to:

$$\hat{\zeta}(\mathbf{k}, t) = - \int_0^t \sin(\omega(k)(t - \tau)) \frac{k \hat{P}_e(\mathbf{k}) e^{-i\mathbf{v} \cdot \mathbf{k}_x \tau}}{\rho \omega(k)} d\tau. \quad (\text{B1})$$

Working out the integral yields:

$$\hat{\zeta}(\mathbf{k}, t) = - \frac{k \hat{P}_e(\mathbf{k})}{\rho \omega(k)} \frac{1}{\omega(k)^2 - (vk_x)^2} \left[e^{-i\mathbf{v} \cdot \mathbf{k}_x t} \omega(k) - \cos(\omega(k)t) \omega(k) + i \sin(\omega(k)t) vk_x \right]. \quad (\text{B2})$$

Now, with $\zeta_d(\mathbf{r}, t)$ being the surface elevation in the ship's frame of reference, we know that $\zeta_d(\mathbf{r}, t) = \zeta(\mathbf{r} + \mathbf{v}t\mathbf{u}_x, t)$, and thus:

$$\hat{\zeta}_d(\mathbf{k}, t) = \hat{\zeta}(\mathbf{k}, t) e^{i\mathbf{v} \cdot \mathbf{k}_x t}, \quad (\text{B3})$$

which yields the result.

Appendix C: Proof of convergence of the wake for linear motion

We first show that the following term in equation (9) vanishes as $t \rightarrow +\infty$ for a sudden uniform linear motion:

$$\zeta_{d,2}(\mathbf{r}, t) = \frac{1}{(2\pi)^2} \iint e^{i\mathbf{k} \cdot \mathbf{r}} \frac{k \hat{P}_e(\mathbf{k})}{\rho(\omega(k)^2 - (vk_x)^2)} e^{i(vk_x + \omega(k))t} d^2\mathbf{k}. \quad (\text{C1})$$

A common trick (see e.g. [25]) to overcome the indefiniteness of the integral above, due to poles sitting on the integration domain, is to take into account the weak viscosity of the fluid ν , which changes the denominator to $\rho(\omega(k)^2 - (vk_x)^2)$ to $\rho(\omega(k)^2 - (vk_x)^2 + i\pi\nu)$ in the equation above, by that shifting the poles of the integrated function off the real axis, and finally take the limit $\nu \rightarrow 0$. For the sake of simplicity, we leave such considerations out of the picture. Changing the variables to polar coordinates (r, φ) yields:

$$\begin{aligned} \zeta_{d,2}(\mathbf{r}, t) &= \frac{1}{(2\pi)^2} \int_{\theta=0}^{2\pi} I(\theta, t) d\theta, \\ \text{with } I(\theta, t) &= \int_{k=0}^{+\infty} \frac{k \hat{P}_e(\mathbf{k})}{\rho(\omega(k)^2 - (vk \cos(\theta))^2)} e^{i\mathbf{k} \cdot \mathbf{r} \cos(\theta - \varphi)} e^{i(vk \cos(\theta) + \omega(k))t} dk. \end{aligned} \quad (\text{C2})$$

Let $f_\theta(k) = vk \cos(\theta) + \omega(k)$. If $\cos(\theta) \geq 0$, then the Riemann–Lebesgue lemma gives that $I(\theta, t) \rightarrow 0$ when $t \rightarrow +\infty$. Whenever $\cos(\theta) < 0$, f_θ has a unique critical point, that we name k^θ . We then use the stationary phase approximation, which gives that $I(\theta, t) = (C/\sqrt{t})\exp(itf_\theta(k^\theta)) + \mathcal{O}(1/t)$, where C is a constant factor involving, among others, $f_\theta''(k^\theta)$. Notably, we still have $I(\theta, t) \rightarrow 0$. We conclude using Lebesgue’s Dominated Convergence Theorem.

We now prove that in the case of any linear motion reaching a final speed v_0 at a finite time t_0 , the wake pattern in the ship’s frame of reference converges to a constant as $t \rightarrow +\infty$. We note $r_0(\tau) = v_0\tau - D$ for $\tau \geq t_0$. As before, we have $\hat{\zeta}_d(\mathbf{k}, t) = \hat{\zeta}(\mathbf{k}, t)e^{iv_0k_x t}$, which enables us to write:

$$\hat{\zeta}_d(\mathbf{k}, t) = -\frac{k\hat{p}_e(\mathbf{k})}{\rho\omega(k)} \left[\int_0^{t_0} \sin(\omega(k)(t-\tau))e^{ik_x(v_0t-r_0(\tau))}d\tau + e^{ik_x D} \int_0^t \sin(\omega(k)(t-\tau))e^{ik_x v_0(t-\tau)}d\tau - e^{ik_x D} \int_0^{t_0} \sin(\omega(k)(t-\tau))e^{ik_x v_0(t-\tau)}d\tau \right]. \quad (\text{C3})$$

The first and the third term can be treated like $\zeta_{d,2}$ above, using the stationary phase approximation. As for the second term, in the Fourier domain, it is none other than $\hat{\zeta}_d$, as given in Eq. (9) (and broke down into five terms), with a factor $e^{ik_x D}$. We have already shown that the corresponding term in the real domain tends to a constant pattern in the ship’s frame of reference, hence the result.